

Validity of the Hadronic Freeze-Out Curve

F Becattini,¹ M Bleicher,² T Kollegger,² M Mitrovski,³
T Schuster,^{2,4} and R Stock^{2,4,*}

¹ Università di Firenze and INFN Sezione di Firenze

² Frankfurt Institute for Advanced Studies(FIAS)

³ Physics Dept., BNL, Brookhaven

⁴ Institut fuer Kernphysik, University of Frankfurt

E-mail: * stock@ikf.uni-frankfurt.de

Abstract. We analyze hadro-chemical freeze-out in central Pb+Pb collisions at CERN SPS energies, employing the hybrid version of UrQMD which models hadronization by the Cooper-Frye mechanism, and matches to a final hadron-resonance cascade. We fit the results both before and after the cascade stage using the Statistical Hadronization Model, to assess the effect of the cascade phase. We observe a strong effect on antibaryon yields except anti- Ω , resulting in a shift in T and μ_B . We discuss the implications for the freeze-out curve.

Hadron production in relativistic A+A collisions is supposed, since Bevalac times [1, 2], to proceed via two separate freeze-out stages. The first, “hadro-chemical” freeze-out fixes the hadronic yields per species, and their ratios, which are conserved throughout the subsequent hadron-resonance cascade expansion. At its end, “kinetic freeze-out” delivers the eventually observed bulk properties such as p_T spectra, HBT correlations, collective flow properties, etc.. Most remarkably, the hadronic yield distributions over species is understood to resemble a grand canonical statistical Gibbs equilibrium ensemble [3, 4], from AGS up to RHIC/LHC energies. Its two most relevant parameters, temperature T and baryochemical potential μ_B , thus capture a snapshot of the system dynamical evolution, taken at the instant of hadro-chemical freeze-out.

In relativistic A+A collisions the thus determined T increases monotonically with $\sqrt{s_{NN}}$, saturating at about 170 MeV (the A+A Hagedorn temperature) while μ_B approaches zero. Systematic statistical model (SM) analysis reveals the “freeze-out curve” [5] in the T, μ_B plane, in which we usually also represent the conjectured plot of the phase diagram of QCD matter.

Such a plot is given in figure 1. It shows two principal lines, firstly a parton-hadron coexistence boundary line, inferred from lattice QCD [6] at low μ_B , and from chiral restoration theory [7] at high μ_B . And, second, the SM freeze-out curve. Remarkably, the lines merge toward $T = 170$ MeV, $\mu_B = 0$. The freeze-out curve locates the QCD hadronization transition temperature T_c : hadronization thus coincides with hadronic freeze-out, here. Equally remarkable, however, the two lines disentangle with increasing

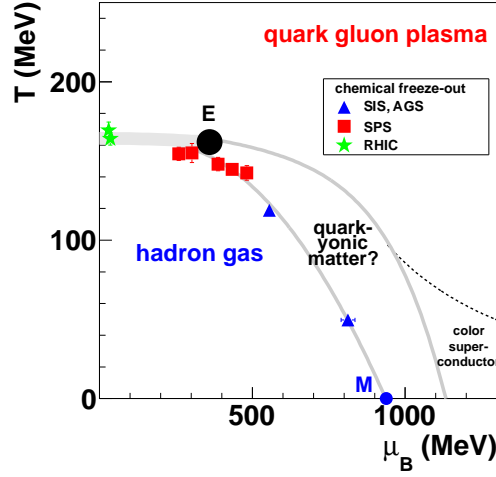


Figure 1. Sketch of the QCD phase diagram, including the hadronic freeze-out curve.

μ_B , becoming spaced by about 30 MeV temperature difference toward $\mu_B = 500$ MeV which corresponds to $\sqrt{s_{NN}} = 5$ GeV in A+A collisions.

What are we freezing out from, here? A phase transition like the parton-hadron transition at small μ_B would offer conditions that establish a grand canonical species equilibrium [8]. Recent ideas concerning a further QCD phase at high μ_B , of quarkyonic matter [9], come to mind. Indicated in figure 1 is a scenario in which the freeze-out curve is identified, tentatively, with a hypothetical quarkyonic matter phase boundary.

Before embarking on this idea a different possible situation needs to be addressed. Taking for granted that the hadron-resonance phase is indeed created at the coexistence curve it might be conceivable that an expansive hadron/resonance evolution stage, setting in at T_c and $\mu_{B,c}$, cools down the population maintaining chemical equilibrium until chemical freeze-out occurs by mere dilution (the inelastic mean free path becoming longer than the system size), at lower T , higher μ_B , thus defining the freeze-out curve.

In this note we test the latter scenario. We employ the framework of the microscopic transport model UrQMD. Its recent hybrid version [10] features a 3+1 hydrodynamic expansion during the high density stage, terminated by the Cooper-Frye hadronization mechanism once the energy density of flow cells falls below a “critical” energy density. This criterion resembles hadronization at the coexistence line of figure 1. The hadron/resonance population can be examined, either, by terminating the evolution at this stage, emitting into vacuum, and fitting the yield distribution by the grand canonical statistical model [11]. Alternatively, the UrQMD hadron/resonance cascade expansion stage is attached, as an “afterburner”. The outcome is again fitted by the SM. Will the afterburner cool the system in equilibrium, to start from T_c and arrive at T on the freeze-out curve?

Figure 2 shows the effect of the final UrQMD cascade stage, in a plot of hadron multiplicities directly after the hydro stage, vs. the multiplicities at the end of the

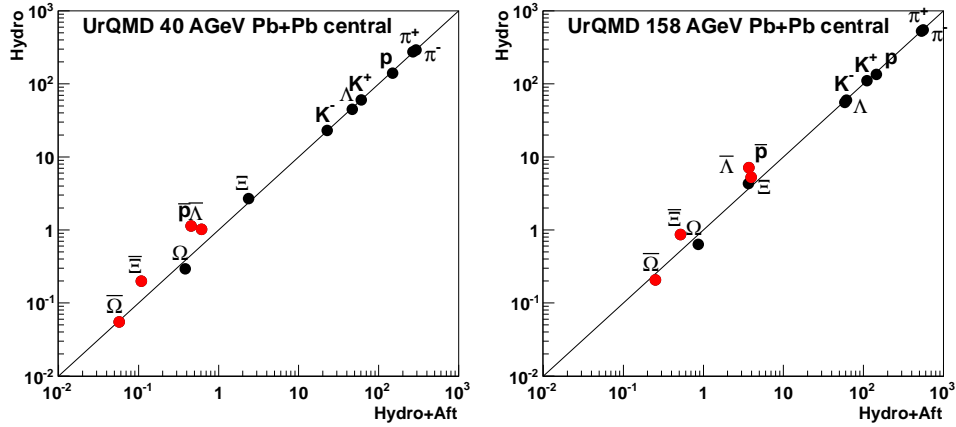


Figure 2. UrQMD calculations for central Pb+Pb at 40A and 158A GeV, plotting the result before the hadronic cascade vs. the result after.

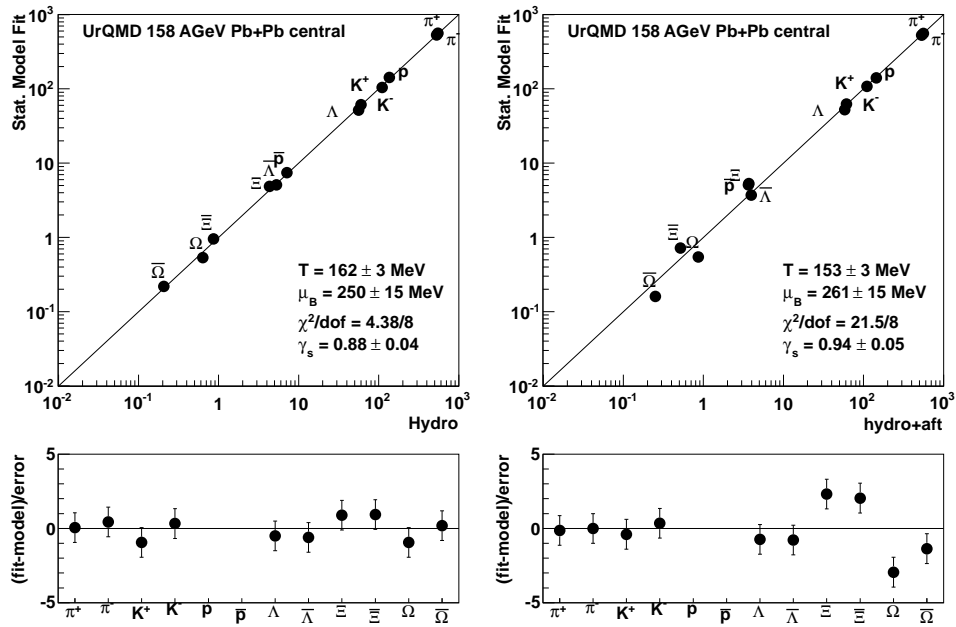


Figure 3. Statistical model fit to UrQMD results for central Pb+Pb at 158A GeV, before and after the cascade stage.

cascade. We illustrate these conditions for central Pb+Pb collisions at the SPS energies 40A and 158A GeV. We see the bulk hadrons unaffected by the afterburner, including the Ξ , Ω and $\bar{\Omega}$. Whereas the other antibaryons, \bar{p} , $\bar{\Lambda}$ and $\bar{\Xi}$, are significantly and selectively suppressed.

Figure 3 illustrates the fits to the hybrid UrQMD results by the statistical model, choosing the 158A GeV case as an example. The afterburner stage indeed shifts (T, μ_B) considerably, from (162, 250) to (153, 261). However, note the dramatic decrease of fit quality, from 4.4 to 21.5 in χ^2 . The effect of the afterburner is, thus, not an in-

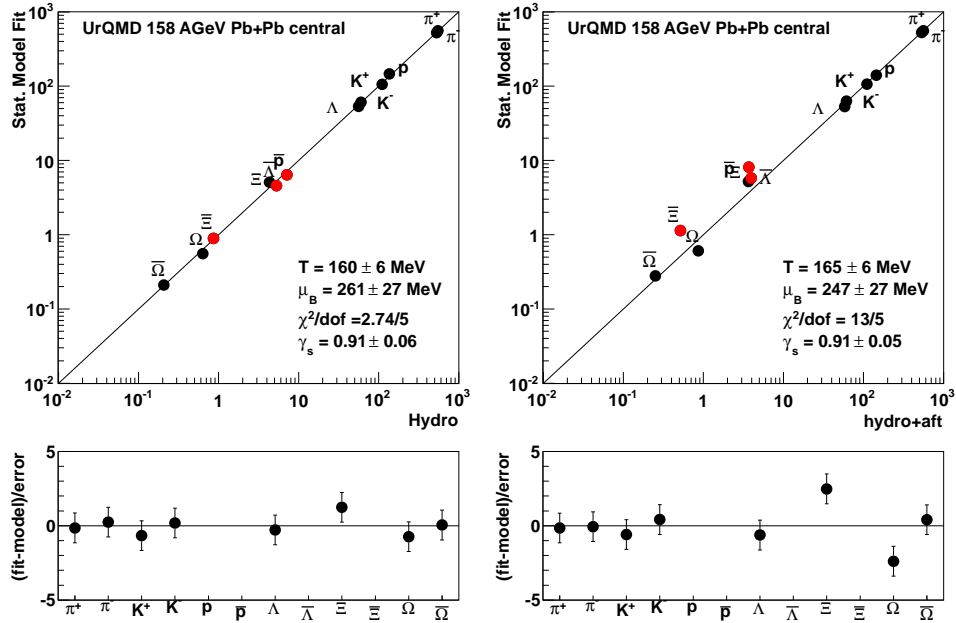


Figure 4. The same as figure 3 except that antibaryons are excluded from the SM fit procedure (but included in the figure).

equilibrium cooling but rather a distortion of the hadron yield distribution, away from equilibrium - as we could guess from figure 2 already. The idea arises to exclude \bar{p} , $\bar{\Lambda}$ and $\bar{\Xi}$ from the SM fit. Figure 4 shows an example, again at 158A GeV. No cooling occurs. The fit to the afterburner output (which features a tolerable χ^2) now ignores the far off-diagonal \bar{p} , $\bar{\Lambda}$ and $\bar{\Xi}$ entries.

We conclude that the hadron/resonance cascade as modelled in the microscopic dynamics of UrQMD can NOT transport an initially established hadrochemical equilibrium from the phase coexistence line of figure 1, down to the freeze-out line. However, it distorts the hadron yield distribution which leads to a downward shift of the freezeout parameters derived from SM analysis, albeit at the cost of rather unsatisfactory χ^2 .

Turning to SM analysis of real SPS data, we note, first, that the χ^2 values obtained from a parallel SM analysis of the NA49 data [12], which are exhibited in figure 1, were also found to be rather high. The idea thus arises to suppose effects in the data, similar to some extent to our UrQMD findings. Figure 5 thus shows a prediction of the SM to the NA49 data at 158A GeV where \bar{p} , $\bar{\Lambda}$ and $\bar{\Xi}$ are excluded from the fit. Very much reminiscent of figure 4 (right), the SM fit here moves up from $T = 158$ MeV (figure 1) to above 170 MeV, at reasonable χ^2 : far above the conventional freeze-out curve at this energy. We shall thus revisit the freeze-out curve at μ_B from about 280 to 430 MeV, obtained, hitherto, from an “unfiltered” application of the statistical model. At the much higher RHIC energies, with μ_B approaching zero, we may expect a smaller such effect of the cascade stage because of the approximate baryon-antibaryon symmetry.

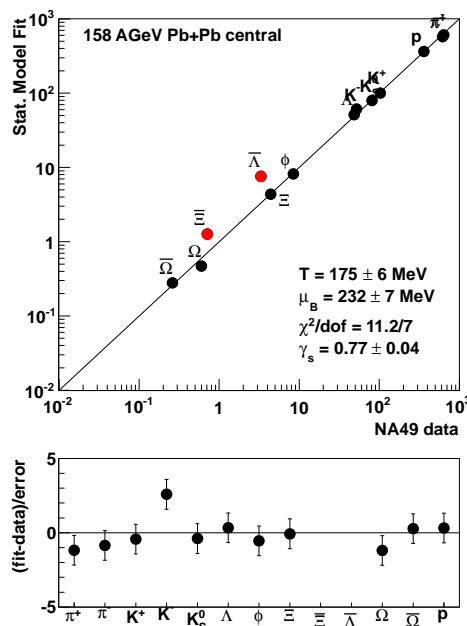


Figure 5. Statistical Model fit to the NA49 data [12] for central Pb+Pb at 158A GeV, omitting the antibaryons except anti- Ω from the fit procedure (their corresponding yields are shown).

References

- [1] I. Montvay, J. Zimanyi, Nucl. Phys. **A316**, 490 (1979).
- [2] R. Stock, Phys. Rept. **135**, 259-315 (1986).
- [3] F. Becattini, M. Gazdzicki, A. Keranen, J. Manninen, R. Stock, Phys. Rev. **C69**, 024905 (2004). [hep-ph/0310049].
- [4] P. Braun-Munzinger, K. Redlich and J. Stachel, in Quark-Gluon Plasma 3, eds. R. C. Hwa and X. N. Wang, World Scientific 2004, p. 491.
- [5] J. Cleymans, H. Oeschler, K. Redlich and S. Wheaton, Phys. Rev. **C73**, 034905 (2006).
- [6] F. Karsch, PoS(Lattice07) 015.
- [7] R. Rapp, T. Schaefer and E. V. Shuryak, Ann. Phys. 280, 35 (2000).
- [8] P. Braun-Munzinger, J. Stachel and Ch. Wetterich, Phys. Lett. B **596**, 61 (2004), R. Stock, [arXiv:0703050, nucl-th].
- [9] L. McLerran and R. Pisarski, Nucl. Phys. A **796** (2007), 83, L. McLerran, [arXiv:0812.1518 [hep-ph]].
- [10] H. Petersen, J. Steinheimer, G. Burau, M. Bleicher, H. Stoecker, Phys. Rev. **C78**, 044901 (2008). [arXiv:0806.1695 [nucl-th]].
- [11] F. Becattini, J. Manninen and M. Gazdzicki, Phys. Rev. C **73** (2006) 044905 [arXiv:hep-ph/0511092].
- [12] https://edms.cern.ch/file/1075059/1/na49_compil.pdf and references therein.